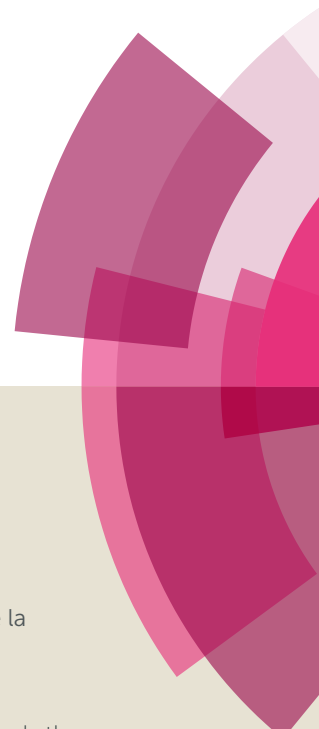
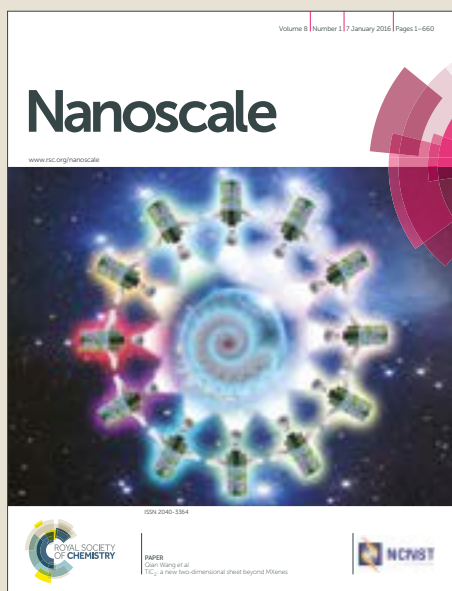


Nanoscale

Accepted Manuscript



This article can be cited before page numbers have been issued, to do this please use: J. L. Paris, P. de la Torre, M. V. Cabañas, M. Manzano, M. Grau, A. I. Flores and M. Vallet-Regí, *Nanoscale*, 2017, DOI: 10.1039/C7NR01070B.



This is an Accepted Manuscript, which has been through the Royal Society of Chemistry peer review process and has been accepted for publication.

Accepted Manuscripts are published online shortly after acceptance, before technical editing, formatting and proof reading. Using this free service, authors can make their results available to the community, in citable form, before we publish the edited article. We will replace this Accepted Manuscript with the edited and formatted Advance Article as soon as it is available.

You can find more information about Accepted Manuscripts in the [author guidelines](#).

Please note that technical editing may introduce minor changes to the text and/or graphics, which may alter content. The journal's standard [Terms & Conditions](#) and the ethical guidelines, outlined in our [author and reviewer resource centre](#), still apply. In no event shall the Royal Society of Chemistry be held responsible for any errors or omissions in this Accepted Manuscript or any consequences arising from the use of any information it contains.

Vectorization of ultrasound-responsive nanoparticles in placental mesenchymal stem cells for cancer therapy

Juan L. Paris^{a,b}, Paz de la Torre^c, M. Victoria Cabañas^a, Miguel Manzano^{a,b}, Montserrat Grau^d, Ana I. Flores^{c,*} and María Vallet-Regí^{a,b,*}

Received 00th January 20xx,
Accepted 00th January 20xx

DOI: 10.1039/x0xx00000x

www.rsc.org/

A new platform constituted by engineered responsive nanoparticles transported by human mesenchymal stem cells is here presented as a proof of concept. Ultrasound-responsive mesoporous silica nanoparticles are coated with polyethylenimine to favor their effective uptake by decidua-derived mesenchymal stem cells. The responsive-release ability of the designed nanoparticles is confirmed, both *in vial* and *in vivo*. In addition, this capability is maintained inside the cells used as carriers. The migration capacity of the nanoparticle-cell platform towards mammary tumors is assessed *in vitro*. The efficacy of this platform for anticancer therapy is shown against mammary tumor cells by inducing the release of doxorubicin only when the cell vehicles are exposed to ultrasound.

Introduction

In the last few years research in nanomedicine is focusing on developing nanocarriers for targeted drug delivery combined with on-demand release behavior.^{1,2} In this sense, porous nanoparticles with great loading capacity and tunable surface properties have become a promising alternative for certain biomedical applications such as cancer therapy. Among those materials, mesoporous silica nanoparticles present high drug adsorption capacity because of their available pores, and they are very robust, which allows further chemical modification of their surface.^{3–5} The release of the transported drugs can be controlled through a stimuli-responsive release that can be achieved through different trigger mechanisms, which can be endogenous, such as changes in pH,⁶ redox potential,⁷ and presence of specific enzymes or analytes;⁸ or exogenous, such as temperature,⁹ light,^{10,11} magnetic fields,^{12,13} electronic fields or ultrasounds.^{14,15}

An ideal nanocarrier for drug delivery in cancer therapy should be capable of specifically targeting tumor tissue avoiding premature release of the payload, and releasing high concentrations of the cargo only at the diseased tissues.^{16–18} Targeted nanoparticles towards tumors can be accomplished

by either passive or active targeting, or by a combination of both.¹⁹ Passive targeting is based on the combination of two features of tumor tissues: high permeability and enhanced retention, in what is called Enhanced Permeation and Retention (EPR) effect.^{20,21} Nanoparticles tend to accumulate in tumor zones due to the abnormal architecture and permeability of the tumor blood vessels. Additionally, there is a poor drainage which results in the retention of the nanoparticles within the tissue.²⁰ On the other hand, active targeting is based on grafting affinity ligands on the surface of nanoparticles able to interact with specific membrane receptors overexpressed by tumor cells, leading to specific retention and uptake by the targeted cancer cells.^{2,19}

However, despite the recent advances in nanoparticles research for biomedicine, the translation of targeted nanocarriers (both passive and active targeting) to the clinic remains to be a challenge.^{22–24} In a totally different approach, cell-based therapies have been investigated as transporters of nanoparticles for cancer treatment.^{25,26} In this sense, Human Mesenchymal Stem Cells are multipotent cells that maintain and regenerate connective tissues, with inherent migratory properties, in response to inflammation and/or injury.^{27–29} This migratory and homing capacities have suggested their use as drug delivery agents for the treatment of isolated and metastatic tumors.^{26,30–32} Conventionally, bone marrow and adipose tissue are the common sources of adult MSCs, although the isolation techniques are invasive and not very efficient in terms of isolated cell quantities.³³ Besides, the donor age strongly influences the number, proliferation and differentiation capabilities, which decline with donor age.³⁴ In the last few years our research group has been investigating an additional source of MSCs from the human decidua of the placenta, which are isolated avoiding invasive procedures.³³ Decidua Mesenchymal Stem Cells (DMSCs) present a number

^a Dpto. Química Inorgánica y Bioinorgánica, Facultad de Farmacia, UCM, Instituto de Investigación Sanitaria Hospital 12 de Octubre i+12, 28040-Madrid, Spain. E-mail: vallet@ucm.es

^b Centro de Investigación Biomédica en Red de Bioingeniería, Biomateriales y Nanomedicina (CIBER-BBN), Spain.

^c Grupo de Medicina Regenerativa, Instituto de Investigación Hospital 12 de Octubre i+12, Madrid, Spain. E-mail: anaisabel.flores@salud.madrid.org

^d Animal Core Facility, Research Center, Instituto de Investigación Hospital 12 de Octubre i+12, Madrid, Spain.

Electronic Supplementary Information (ESI) available: Characterization of Mesoporous Silica Nanoparticles, *in vivo* fluorescence, cytotoxicity assays. See DOI: 10.1039/x0xx00000x

of advantages over conventional MSCs, such as: they are very easy to obtain without invasive techniques; they constitute a homogeneous population with high proliferation and differentiation capacities; they are adult stem cells from the maternal part of the placenta, with low or non-immune response and genetically stable during expansion.³³ Additionally, DMSCs present migratory properties towards tumors, both *in vitro* and *in vivo*, and, additionally, they inhibit the growth of primary tumors and the development of new tumors.³⁴ Consequently, DMSCs seem to be excellent carriers of pharmaceutical agents towards tumor tissues. However, if the cells are carrying cytotoxic agents, some strategy should be developed to ensure DMSCs survival during transport. An interesting approach would consist of loading the cytotoxic cargo on stimuli-responsive nanoparticles for drug delivery. Those smart nanocarriers would be introduced into the DMSCs, which would transport them to the targeted tissue. The application of an external stimulus would trigger the release of the cytotoxic drug. As a consequence, the drug would have to be released from the DMSCs to the surrounding tissue.^{26,35} The process by which hydrophobic cytotoxic molecules (like doxorubicin)^{36,37} can diffuse out of a transporting cell to kill surrounding cancer cells has been called the "bystander effect".³⁸⁻⁴⁰

In this manuscript we have developed a proof of concept cell-platform constituted by engineered ultrasound-responsive nanoparticles which are vectorized to tumor tissues by using DMSCs. The nanocarrier provides a controlled release, triggering the payload release on demand when a penetrating stimulus such as Ultrasounds would be applied. To the best of our knowledge this is the first time that human mesenchymal stem cells are employed as transporters that can release a therapeutic molecule on-demand.

Results and discussion

Engineered Ultrasound-Responsive Nanoparticles

Ultrasound-Responsive Nanoparticles (UR-NPs) are composed of an ultrasound (US) responsive copolymer (poly(2-(2-methoxyethoxy)ethylmethacrylate-co-2-tetrahydropyranil methacrylate, p(MEO₂MA-co-THPMA)), covalently grafted to the surface of MCM-41 type Mesoporous Silica Nanoparticles. The synthesis, characterization and behavior of these hybrid nanoparticles has been previously reported.¹⁵ The material presents negatively charged surface at the pore walls, due to the silanol groups, which permits to load a high amount of the cytotoxic drug doxorubicin within the pores.^{41,35} Then, the pores are closed with a responsive polymeric gate to avoid premature release. The application of an exogenous stimulus, such as ultrasound, enables the delivery of the maximum amount of drug possible.

We have developed a cell-platform to transport the UR-NPs selectively to tumor tissues. Once in the tumor, the cytotoxic agent would be released, damaging the cancer cells without affecting healthy tissues. In this combined approach, the NPs will provide the responsive drug release, while the

biological component (DMSCs) will act as a specific vehicle to carry the NPs to the tumor. To obtain this goal, the nanoparticles must be internalized into the cell vehicles. Cellular uptake is generally enhanced employing internalization ligands or positively charged moieties on the surface of NPs.⁴² In this sense, polyethylenimine (PEI) is a synthetic cationic polymer that has been widely used to deliver oligonucleotides, siRNA and plasmid DNA to cells.^{43,44} An interesting approach for effectively NPs internalization into cells consists on decorating the NPs surface with PEI. Cellular uptake of PEI-coated nanoparticles relies on the electrostatic interaction between the positively charged polymer and negatively charged cell membrane, in a charge-dependent mechanism that is not selective on the cell type.⁴³ The above synthesized UR-NPs were coated with 1800 Da PEI (UR-NPs@PEI), which is known to present low cytotoxicity, to confere a positive charge on their external surface that will increase the amount of NPs internalized in DMSCs.³⁵

The presence of PEI in the particles was confirmed by different techniques: the Zeta Potential changed from negative to positive values after PEI coating (Figure 1). Thermogravimetric Analysis (TGA) data showed an organic matter percentage for the UR-NPs of 25 %, and 40 % for UR-NPs@PEI, what indicated an estimate of 15 % of PEI in the final material. BET surface area decreased from 180 m² g⁻¹ for UR-NPs to 70 m² g⁻¹ for UR-NPs@PEI. Small angle X-ray diffraction patterns show that hexagonal pore order of the mesoporous silica nanoparticles was maintained (see Figure S1). The diameter and morphology of the NPs remains unmodified after the PEI coating, as it can be seen in the Scanning Electron Microscopy images (Figure 1). The mesoporous order can be appreciated in the Transmission

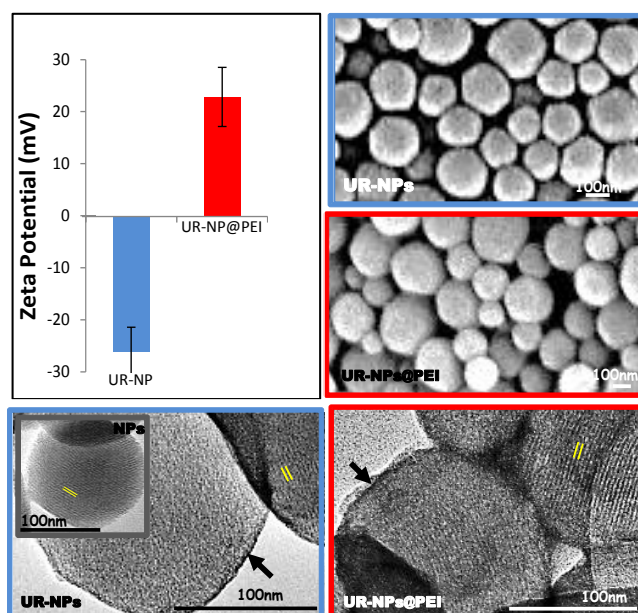


Figure 1. Characterization of Ultrasound-responsive nanoparticles with or without PEI coating: Zeta potential values (top, left), Scanning Electron Microscopy micrographs of UR-NPs and UR-NPs@PEI (top, right), Transmission Electron Microscopy micrographs of Phosphotungstic acid-stained non-Ultrasound responsive NPs, UR-NPs and UR-NPs@PEI (bottom). Arrows indicate the presence of a polymeric coating, parallel segments indicate the ordered mesochannels.

Electron Microscopy micrographs which also showed the presence of the US-responsive copolymer, or the copolymer plus the PEI, on the external surface of the mesoporous ordered NPs when the materials were stained with Phosphotungstic acid (Figure 1). As it will be seen throughout this article, nanoparticles labeled with different dyes have been employed, and their characterization did not show any significant differences when compared to the non-labeled nanoparticles. Several cargo molecules have also been loaded within the mesopores, in order to evaluate various aspects of the materials US-responsiveness.

The US-responsiveness of UR-NPs@PEI was evaluated initially *in vial*, with a fluorescein release experiment. Taking into account that the gatekeeper copolymer shows a dual temperature-US responsiveness,¹⁵ fluorescein loading in UR-NPs was performed at 4 °C. Under these conditions the polymer that acts as gatekeeper presented an open or hydrophilic conformation. After the dye loading process, the temperature was increased to 50 °C, inducing the copolymer to collapse, i.e. change to a hydrophobic conformation, closing the pore entrances. Then, loaded UR-NPs were coated with PEI. Dye release experiments (Figure 2) show that the behavior of the UR-NPs@PEI was similar to that of UR-NPs without coating; the presence of PEI coating did not induce any significant differences in the maximum percentage of fluorescein released with or without ultrasound (which was already reached after 16 h).¹⁵ As commented above, before US application, the polymeric gate is collapsed at the nanoparticle surface, blocking the pores and preventing cargo release. After insonation, one of the monomers in the polymeric gate (THPMA) is cleaved, yielding hydrophilic methacrylic acid. This change in the copolymer structure induces an increase in its hydrophilicity, triggering a change of conformation towards coil-like, which allows drug release from the material. The evaluation of this change in the polymeric gate has been demonstrated in our previous work.¹⁵ Here, we show that these engineered nanoparticles continue to behave as stimulus-responsive drug nanocarriers even though they have been coated with PEI.

In vivo ultrasound-responsiveness of this material was checked loading Calcein-AM into UR-NPs@PEI. Calcein-AM is a low-fluorescent indicator that can be converted *in vivo* to

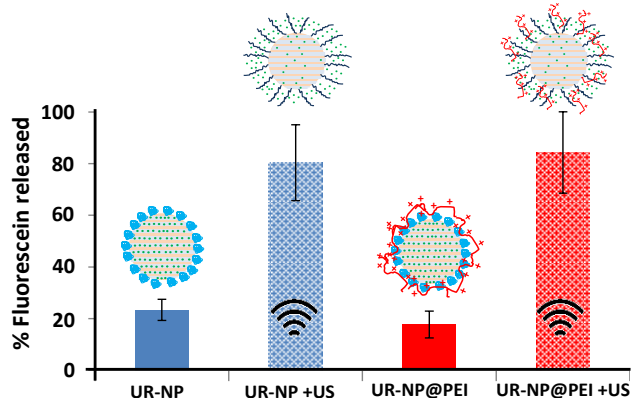


Figure 2. Percentage of fluorescein released in PBS at 37 °C from UR-NPs and UR-NPs@PEI with or without Ultrasound exposure after 16 h.

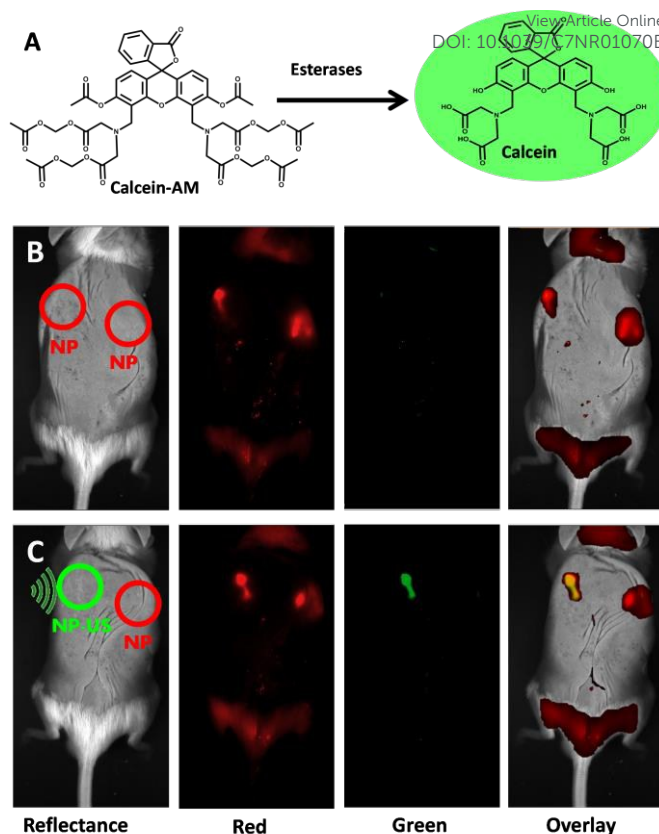


Figure 3. Data showing the material cargo retention and release capability *in vivo*. *In vivo* fluorescence of subcutaneously injected UR-NPs@PEI (red channel) and the released cargo (green channel); Scheme of green fluorescence generation by the cleavage of cargo molecule (Calcein-AM) after release, yielding fluorescent Calcein (A); *In vivo* fluorescence images of the different fluorescence channels before (B) and 100 min after ultrasound application (1 MHz, 10 min, 3 W cm⁻²) (C).

highly-fluorescent Calcein due to the activity of esterases in the surrounding cells (Figure 3A). The Calcein-AM loaded material was injected subcutaneously and bilaterally in mice, monitoring the *in vivo* fluorescence before and after US application on one of the injection sites (Figure 3B-C). In order to point the location of the nanoparticles, Rhodamine B-labeled UR-NPs@PEI were used for these experiments. Figure 3B, corresponding to the fluorescence before US application, shows red fluorescence, delimiting the location of NPs due to the Rhodamine B labeling. No fluorescence was observed in the green channel (therefore, there had been no cargo release). After US application (1 MHz, 3 W cm⁻², 10 min), red fluorescence indicated that the NPs were still present at the injection site and green fluorescence appeared only in the US-exposed area (Figure 3C). Taking into account that Calcein-AM inside the material pores is not accessible to the esterases from the cells, the presence of green fluorescence indicates that Calcein-AM was released from the material when the gatekeeper was opened due to ultrasound exposure. On the other hand, at the injection site without US application, there was no green fluorescence, which indicates that Calcein-AM is retained inside the nanoparticle pores and not exposed to esterases. The progressive increase of green fluorescence *in vivo* at different time points after ultrasound application can be seen in Figure S2. These results demonstrate the capability

of the UR-NPs@PEI to retain a cargo and release it when exposed to ultrasound *in vivo*.

Ultrasound-Responsive Nanoparticles-Cell Platform

After evaluating the *in vitro* and *in vivo* responsiveness of UR-NPs@PEI, we tested the interaction of the UR-NPs@PEI with the DMSCs which will act as transporters to the tumor tissue. To do so, the effect of UR-NPs@PEI at different concentrations on DMSCs viability was tested using the MTS and LDH assays (Figure S3). The results show no toxicity up to $200 \mu\text{g mL}^{-1}$, and a small toxicity at higher concentrations. Therefore, a concentration of $200 \mu\text{g mL}^{-1}$ was chosen for further experiments.

Then, DMSCs were exposed to UR-NPs@PEI to study their internalization and retention in the cells. For these studies, the NPs were covalently labeled with Fluorescein isothiocyanate (FITC). **Figure 4A-C** shows the fluorescence microscopy images of DMSCs stained with DAPI (nuclei) and Alexa Fluor[®]568 phalloidin (cytoplasm) after incubation with labeled Nanoparticles ($200 \mu\text{g mL}^{-1}$ for 2 h). As expected, microscopy images indicate that UR-NPs@PEI were internalized by the cells better than UR-NPs (Figure 4A-B). Moreover, the UR-NPs@PEI escaped the endo-lysosomal compartment shortly after endocytosis, since NP fluorescence (green) and lysosomes (red) do not colocalize (Figure 4C). This behavior can be attributed to the Proton Sponge Effect provided by PEI.⁴³ Under the acidic conditions of the lysosome, PEI (and other polycationic molecules) presents a very high positive charge. This induces the entrance in the lysosomes of chloride anions, accompanied by water. The lysosomes swell until they eventually burst, releasing their contents into the cytoplasm. The quantification of UR-NPs@PEI uptake ($200 \mu\text{g mL}^{-1}$ for 2 h) by DMSCs by Flow Cytometry indicates a more successful internalization of UR-NPs@PEI compared to the nanoparticles

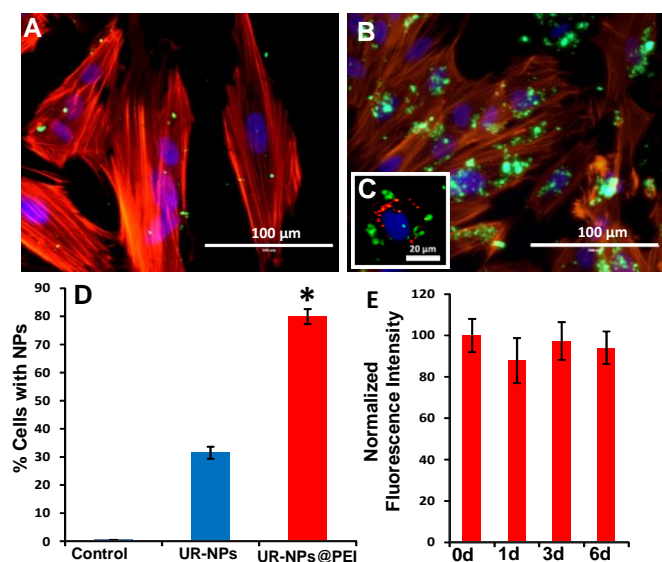


Figure 4. Fluorescence microscopy images of NP-loaded DMSCs; blue (nucleus), red (cytoplasm), green (NPs): UR-NPs (A), UR-NPs@PEI (B); Colocalization study of UR-NPs@PEI (green), nucleus (blue) and lysosomes (red) in DMSCs 2 h after internalization (C); Flow-cytometry data regarding UR-NPs and UR-NPs@PEI uptake (D); Flow-cytometry data regarding UR-NPs@PEI retention (E) (Data are Means \pm SD, N = 3, * $p < 0.05$).

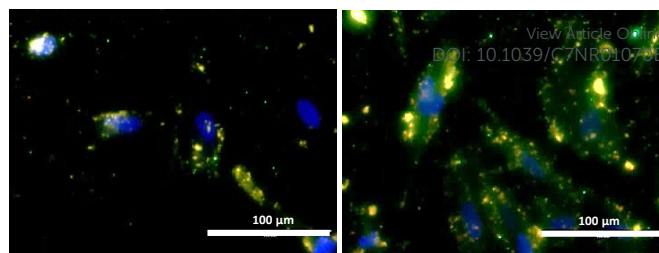


Figure 5. Fluorescence microscopy images of DMSCs incubated with RhodamineB-labeled UR-NPs@PEI loaded with fluorescein before (left) and after (right) ultrasound irradiation. Overlay images of three fluorescence channels: Blue fluorescence (nuclei), red fluorescence (UR-NPs@PEI) and green fluorescence (fluorescein cargo). Fluorescence microscopy images taken 30 min after the US exposure was performed.

without PEI (Figure 4D, Figure S4). The coated particles were also retained inside the cells for at least 6 days (Figure 4E), enough for the cells to reach the tumor, according to our previous work.³⁵

In addition, the UR-NPs@PEI retain their cargo after uptake by the DMSCs and are also able to release intracellular fluorescein after US application (**Figure 5**). For this experiment, Rhodamine B-labeled nanoparticles were used to simultaneously study the location of UR-NPs@PEI (red fluorescence) and their cargo (green fluorescence). Before US exposure, red and green fluorescence colocalize, indicating that the dye is retained inside UR-NPs@PEI. After insonation (1MHz , 3W cm^{-2} , 5 min), a significant part of the dye diffuses out of the NPs and stains the cell cytoplasm (images taken 30 min after insonation), as a consequence of the polymeric gates changing from a closed to an open conformation (Figure 2).

The above results show the possibility to fabricate a cell platform containing US-responsive NPs inside the DMSCs for at least 6 days. To evaluate the effect of the cell-platform as transporters of cytotoxic molecules, the UR-NPs@PEI were loaded with doxorubicin (loaded amount was $2.94 \pm 0.17 \%$). First, we incubated different concentrations of cytotoxic-loaded NPs with the DMSCs for 2 h. After that, we washed the cells to eliminate the non-internalized NPs and cell viability was evaluated after 24 and 72 h (**Figure 6**). No toxicity was

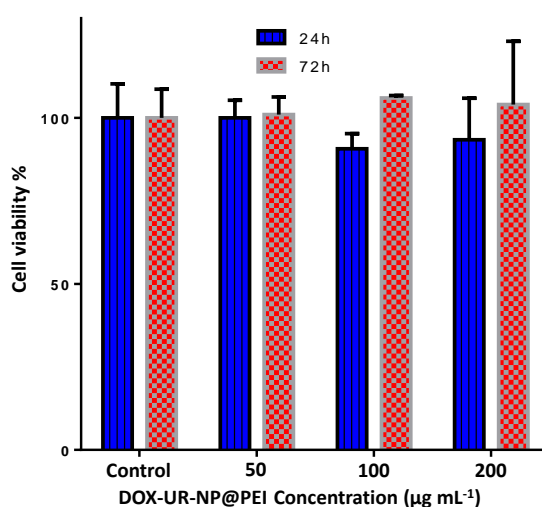


Figure 6. Cytotoxicity assay in DMSCs of Doxorubicin-loaded UR-NPs@PEI at different concentrations after 24 h and 72 h measured by Alamar Blue test. No significant differences were found at any of the tested concentrations.

observed up to a concentration of $200 \mu\text{g mL}^{-1}$. Therefore, these conditions ($200 \mu\text{g mL}^{-1}$ UR-NPs@PEI for 2 h) were used for any further experiments. It is worth noting that, in our previous work, we had observed significant toxicity in DMSCs 48 h after internalization caused by similar doxorubicin-loaded NPs but without stimulus-responsive gatekeeper.³⁵ Thus, the NPs engineered in the present work are capable of retaining the cytotoxic drug inside them, preventing a premature leakage of the doxorubicin that could damage the transporting cells before they reach their target tissue.

The next stage was to check the capability of the cell-NPs platform to reach the tumor site. In this sense, we performed a standardized *in vitro* cell migration assay towards the tumor homogenate to check if the presence of UR-NPs@PEI inside the cells has any negative impact in the DMSCs migration capacity. The results showed a high migration capacity of DMSCs towards tumor homogenate, which was maintained in our Platform carrying UR-NPs@PEI, even if those NPs were loaded with doxorubicin (DOX-Platform) (Figure 7). The amount of doxorubicin transported by the DOX-Platform was determined to be $0.47 \pm 0.08 \mu\text{g}$ of doxorubicin per 10000

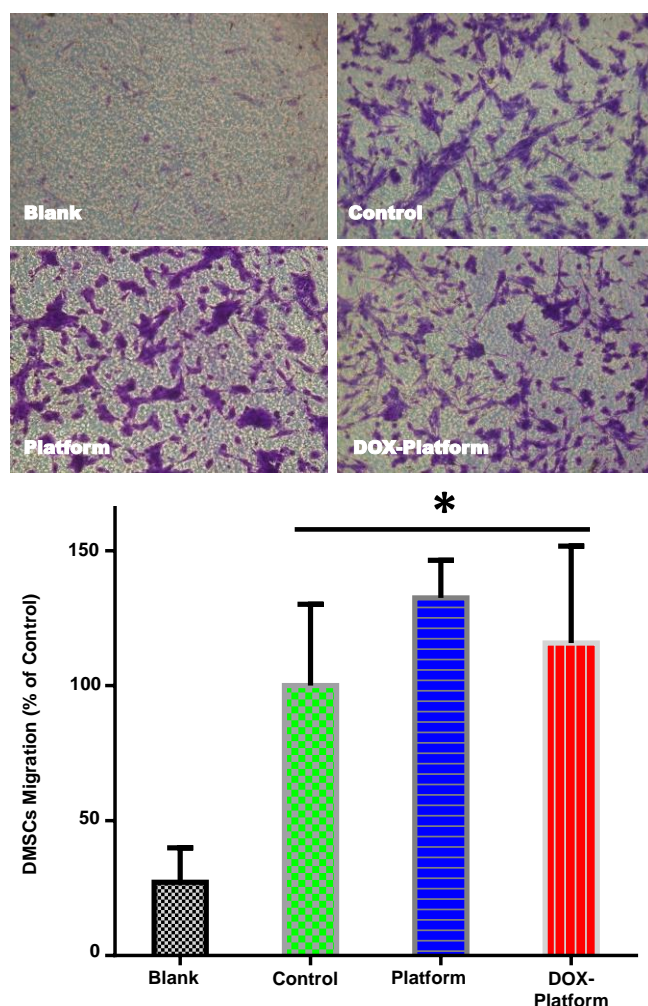


Figure 7. *In vitro* Transwell® migration assay of DMSCs against culture medium (basal), tumor homogenate (control) and migration of DMSCs loaded with UR-NP@PEI or DOX-UR-NP@PEI against tumour homogenate. Optical microscopy images of migrated cells (top) and quantification of migrated cells by UV-Vis spectrophotometry (bottom) (Mean \pm SD, N = 3, *p < 0.05).

DMSCs. The quantification of migrated cells shows no significant difference in cell migration due to UR-NP@PEI (with or without doxorubicin). These data indicate that stimulus responsive NPs containing a cytotoxic drug can be vectorized to the tumor site by DMSCs.

Finally, in order to test whether this developed platform (UR-NPs@PEI inside DMSCs) could be useful for anticancer therapy, an *in vitro* co-culture experiment was carried out. The transporting cells (DMSCs and DOX-Platform) were divided in two groups and half of the samples were exposed to US (1 MHz, 3 W cm^{-2} , 5 min). Then, the DMSCs and DOX-Platforms with/without US exposure were seeded in a Transwell® culture insert on top of a well that contained NMU cancer cells (DMSCs:NMU ratio was 1:2). After 24 and 48 h, the Transwell® inserts were removed and the NMU viability was evaluated by Alamar Blue test. Figure 8 shows that NMU cell viability is only affected when US is applied on DMSCs carrying doxorubicin-loaded UR-NPs@PEI, but it remains unaffected in any of the other experimental conditions. Therefore, doxorubicin remains retained in UR-NPs@PEI inside DMSCs until the platform is exposed to US. After insonation, the nanoparticles release their cargo, which can diffuse towards tumor cells, inducing their death. Furthermore, that effect appears to be dose-dependent, since the reduction in NMU cell viability is smaller when the ratio DMSC:NMU is 1:5 (Figure S5).

These results show the possibility to introduce cytotoxic-loaded stimulus-responsive NPs in DMSCs as cell carriers. The migratory capacity of these cells to the tumor tissue was maintained in presence of UR-NPs. This platform was activated, i.e. released the cytotoxic drug, just when an external stimulus was applied, in principle, when the cell platform reached the tumor tissue.

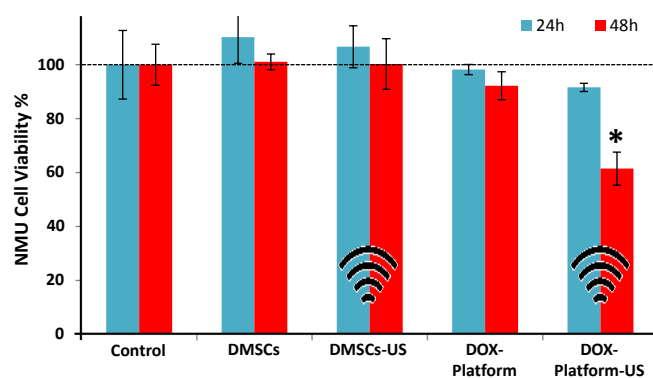


Figure 8. Cytotoxicity assay of NMU cells after co-culture with DMSCs or with DOX-Platform (with or without Ultrasound application) measured by Alamar Blue test. DMSCs to NMU ratio was 1:2. (Mean \pm SD, N = 3, *p < 0.05).

Conclusions

A cell platform to transport ultrasound-responsive nanoparticles towards tumor tissue has been developed. Experiments, both *in vial* and *in vivo*, have demonstrated the ultrasound responsiveness of the system, showing the capability to induce cargo release on-demand. These polyethylenimine-coated nanoparticles were efficiently

internalized by decidual-derived mesenchymal stem cells and they were retained for at least 6 days. The nanoparticle-cell construct also presented ultrasound-responsive cargo release capability.

The tumor-tropic behavior of the cells was preserved when transporting doxorubicin-loaded nanoparticles. This doxorubicin carrying platform was able to induce the death of mammary cancer cells *in vitro* when it was exposed to ultrasound.

The obtained results indicate that this platform could be employed to transport cytotoxic drugs specifically to tumors, and release them when exposed to ultrasound.

Experimental section

Reagents and Characterization Techniques.

Following compounds were purchased from Sigma-Aldrich Inc.: Ammonium nitrate, cetyltrimethylammonium bromide (CTAB), tetraethyl orthosilicate (TEOS), methacrylic acid (MAA), pyridine, p-toluenesulfonic acid, toluene, dichloromethane (DCM), dihydropyran, dimethylformamide (DMF), 2-(2-methoxyethoxy) ethylmethacrylate (MEO₂MA), 4,4'-Azobis(4-cyanovaleric acid) (ABCVA), diethylether, N,N'-dicyclohexylcarbodiimide (DCC), N-hydroxysuccinimide (NHS), phosphate-buffered solution (PBS), fluorescein sodium salt, polyethylenimine (PEI) of 1800 Da, rhodamine-B isothiocyanate and fluorescein isothiocyanate (FITC). Calcein-AM was purchased from ThermoFisher Scientific. DMEM, penicillin-streptomycin, non-essential amino acids, trypsin-EDTA were purchased from Invitrogen (Fisher Scientific, Madrid, Spain). Fetal bovine Serum is from Biowest (labClinics, Spain). Trans-well were purchased from Nunc (Fisher Scientific, Spain). These compounds were used without further purification. Tetrahydropyranyl methacrylate (THPMA) was synthesized as described previously.^{15,45}

The materials were analyzed by X-ray diffraction (XRD) in a Philips X-Pert MPD diffractometer equipped with Cu K α radiation. Thermogravimetry and Differential Thermal Analysis (TGA/DTA) were performed in a Perkin Elmer Pyris Diamond TG/DTA analyzer, with 5 °C min⁻¹ heating ramps, from room temperature to 600 °C. Fourier Transformed Infrared (FTIR) spectra were obtained in a Nicolet (Thermo Fisher Scientific) Nexus spectrometer equipped with a Smart Golden Gate ATR accessory. Surface morphology was analyzed by Scanning Electron Microscopy (SEM) in a JEOL 6400 Electron microscope. Transmission Electron Microscopy (TEM) was carried out with a JEOL JEM 2100 instrument operated at 200 kV, equipped with a CCD camera (KeenView Camera). Phosphotungstic acid staining was employed to detect the presence of organic matter in the hybrid materials. N₂ adsorption was carried out on a Micromeritics ASAP 2010 instrument; surface area was obtained by applying the Brunauer-Emmett-Teller (BET) method to the isotherm and the pore size distribution was determined by the Barrett-Joyner-Halenda (BJH) method from the desorption branch of the isotherm. The mesopore size was determined from the

maximum of the pore size distribution curve. The Z-potential was measured in deionized water by means of a Zetasizer Nano ZS (Malvern Instruments) equipped with a 633 nm "red" laser.

Engineered US-Responsive Nanoparticles.

Preparation of UR-NPs. A detailed description of the Ultrasonic-Responsive Nanoparticles (UR-NPs) synthesis method can be found in our previous work.¹⁵ Mesoporous silica nanoparticles were fabricated by the modified Stöber method from TEOS in the presence of CTAB as structure-directing agent under basic and very dilute conditions.

The random copolymer, poly(2-(2-methoxyethoxy)ethylmethacrylate-co-2-tetrahydropyranyl methacrylate, p(MEO₂MA-co-THPMA), was synthesized by free radical polymerization from 2-(2-methoxyethoxy) ethylmethacrylate, MEO₂MA, and 2-tetrahydropyranyl methacrylate, THPMA, in a MEO₂MA:THPMA ratio of ca. 90:10. The synthesis was performed at 80 °C overnight in DMF solution under inert atmosphere.

Grafting the polymer nanogate to mesoporous silica nanoparticles to obtain UR-NPs was performed in two steps. First, the previously copolymer, p(MEO₂MA-co-THPMA), was modified with an alkoxy silane (3-aminopropyl triethoxysilane) through DCC-NHS chemistry. Then, the silylated polymer was grafted to the silica nanoparticles surface through sol-gel chemistry. A ratio polymer:nanoparticles of 6:1 was used, and the silylated polymer was added in 3 steps to the nanoparticles.¹⁵

FITC and Rhodamine B-labeled UR-NPs were prepared following the same procedure but using NPs covalently labeled with the fluorophore during NP synthesis as described elsewhere.^{15,35}

Preparation of UR-NPs@PEI. The synthesis of stimuli responsive nanoparticles coated with PEI (UR-NPs@PEI) was carried out by adding 5 mg of PEI to 10 mg of UR-NPs dispersed in 2 mL of PBS. The coating was carried out at 37 °C for 3 h. The product was washed several times with PBS, centrifuged and dried under a vacuum at 25 °C.

Cargo loading and release. *Cargo loading:* 20 mg of UR-NPs were placed in a glass vial with a septum and dried at 80 °C under vacuum for 24 h. Then, the vial was placed at 4 °C with magnetic stirring and 5 mL of cargo solution (20 mg mL⁻¹ fluorescein in PBS) were added and the suspension was stirred for 24 h. After that time, the sample was filtered and washed twice with warm PBS (50 °C) to remove the potential fluorescein absorbed on the external surface. Note that the cargo loading was performed at 4 °C, below than the lower critical solution temperature (LCST) which means that the polymer presents an extended conformation (pores opened). After loading, the temperature was increased to 50 °C (above the LCST) which induces the polymer to collapse, closing the pore entrances.¹⁵ After that, loaded UR-NPs were coated with PEI in a similar way to that above described.

In vial cargo Release: 9 mg of fluorescein-loaded nanoparticles were suspended in 1.8 mL of PBS pH 7.4 (10

mM). Then, 0.5 mL of that UR-NPs suspension were placed on a Transwell® permeable support with 0.4 µm of polycarbonate membrane (3 replicas were performed). The well was filled with 1.5 mL of PBS and the suspension was stirred at 37 °C and 100 rpm during all the experiment. For the US experiments the particles suspension was subjected to US exposure (10 min at 1.3 MHz and 100 W) before placing it on the Transwell® insert. The amount of fluorescein released after 16 h was determined by fluorescence spectrometry (λ_{exc} 490, λ_{em} 514 nm).

In vivo evaluation of US Responsive Nanoparticles

The *in vivo* US-responsiveness of UR-NPs@PEI was evaluated on a mouse model (FVB strain). Mice were shaved and depilatory cream was employed to remove their hair in the area that was evaluated (to prevent auto-fluorescence and to apply the ultrasound gel). Nanoparticles were covalently labeled with Rhodamine B, as previously mentioned, to be able to visualize the NPs by *in vivo* fluorescence imaging (*In vivo Xtreme*®, Bruker). Loading of Calcein-AM was performed following the same procedure as previously described but using a 2 mg mL⁻¹ solution of the cargo in a mixture of DMSO and PBS (the material was washed several times with PBS after cargo loading). Calcein-AM loaded nanoparticles were injected subcutaneously and bilaterally in mice (2 mg of NPs in 100 µL PBS per injection). US was applied at the left injection site (1 MHz, 3 W cm⁻², 10 min continuous application) and using ultrasound gel. *In vivo* fluorescence was evaluated at different wavelengths (Green: λ_{exc} 490, λ_{em} 514 nm, Red: λ_{exc} 540, λ_{em} 625 nm), before and after US application.

Ultrasound-Responsive Nanoparticles-Cell Platform

Human placentas from healthy mothers were obtained from the Department of Obstetrics and Gynecology under written informed consent approved by the Ethics Committee from Hospital Universitario 12 de Octubre, Madrid, Spain. Processing of placental membranes and culture of primary cells (DMSCs) were done as previously reported.^{33,34}

Cellular uptake of Nanoparticles. DMSCs were plated 24 h before starting the experiment in culture multiwell plates at a density of 10⁴ cells per cm². After incubation with particles (UR-NPs and UR-NPs@PEI) in serum-free culture medium (200 µg mL⁻¹) for 2 h, the media were removed and the cells were washed with PBS three times. Then, the cells were fixed with Z-fix solution (Anatech, USA) for 15 min, permeabilized with 0.1 % Triton X-100 in PBS at room temperature for 5 min and, subsequently incubated for 20 min with Alexa Fluor®568 phalloidin (Invitrogen, Spain) for staining F-actin. DAPI (4',6-diamidino-2-phenylindole) at 1 µg mL⁻¹ was used to stain and visualize the nuclei. Fluorescence microscopy was performed with an Evos® FL Cell Imaging System equipped with tree Led Lights Cubes (λ_{exc} (nm); λ_{em} (nm)): DAPI (357/44; 447/60), GFP (470/22; 525/50), RFP (531/40; 593/40) from AMG (Advance Microscopy Group). Quantitative analysis of cellular uptake was performed by flow cytometry (FACS). 200 µg mL⁻¹ particles were incubated with the DMSCs for 2 h, and then removed by washing three times with PBS. Subsequently, the

cells were trypsinized, collected by centrifugation and redispersed in PBS solution with trypan blue (0.5 %) to remove extracellular fluorescence. The fluorescence intensity of 10,000 cells was quantified by FACS. Statistical analysis for differences between groups was carried out by the Student's t test.

Quantitative analysis of particle retention was performed by FACS. Particles at a concentration of 200 µg mL⁻¹ were incubated with the DMSCs for 2 h, and then removed by washing three times with PBS. The cells were then cultured in fresh medium for indicated time points. Subsequently, the cells were collected by trypsinization and centrifugation, and redispersed in PBS solution with trypan blue (0.5 %). The fluorescence intensity of 10,000 cells was quantified by FACS. The fluorescence intensities obtained after the first day were corrected by the cell dilution folds due to cell division.

Cytotoxicity of Nanoparticles. The cytotoxicity of both, UR-NPs and UR-NPs@PEI, was evaluated using the following standard protocols:

Lactate dehydrogenase (LDH) activity test: Extracellular LDH activity was measured in the media using the kit for Quantitative determination of LDH (Spinreact, Spain). DMSCs were incubated with different sets of NPs for 2 h at different concentrations in serum-free DMEM (n=3). Then, the media were changed with fresh complete culture media and the cells were incubated for another 24 h. The culture medium was then collected to determine the extracellular LDH activity, measured by means of a spectrophotometer (at 340 nm) following the manufacturer's protocol.

MTS(3-(4,5-dimethylthiazol-2-yl)-5-(3-carboxymethoxyphenyl)-2-(4-sulfophenyl)-2H-tetrazolium) assay: The MTS reduction assay was performed using a commercial assay and following the manufacturer's protocol (CellTiter® Aqueous One Solution Cell Proliferation Assay). Briefly, DMSCs were incubated with various concentrations of NPs for 2 h in serum-free DMEM (n=3). Then, the media were changed with fresh complete culture media and the cells were incubated for another 24 h. The medium was replaced with 600 µL culture medium including MTS, and the incubation proceeded for 3 h. The medium was then removed, and its absorption at 490 nm was measured using a spectrofluorimeter plate reader (EnSpire, PerkinElmer).

Intracellular fate of Nanoparticles. For the co-localization of NPs and lysosomes, the cells were incubated with 200 µg mL⁻¹ particles for 2 h. The cells were washed twice with PBS solution. Then, lysosomes were stained with the Cell Tracker® Lysosome staining kit following the manufacturer's protocol (AAT Bioquest, Inc, USA). After washing twice with PBS, fresh medium was added. The cells were fixed and stained with DAPI as previously described. Fluorescence microscopy was performed with an Evos® FL Cell Imaging System.

In vitro evaluation of Ultrasonic Responsive cell platform. Preparation of UR-NPs@PEI containing Doxorubicin was performed by stirring 10 mg of UR-NPs in 5 mL of a solution of doxorubicin in PBS (1 mg mL⁻¹) for 24 h at 4 °C. Doxorubicin-loaded particles were washed by centrifugation and redispersion in PBS at 50 °C several times. Loaded

nanoparticles were coated with PEI as previously described (DOX-UR-NPs@PEI). Quantification of doxorubicin inside DOX-UR-NPs@PEI was performed by dispersing a known amount of nanoparticles in 95% ethanol in an ultrasonic bath to force the release of the cargo, and measuring the fluorescence of doxorubicin in ethanolic solution after filtration of the nanoparticles. A calibration curve of doxorubicin fluorescence in ethanolic solution (λ_{exc} 470, λ_{em} 585 nm) was used.

The preparation of the engineered cell-NPs platform was carried out by the following procedure: DMSCs were incubated with 200 $\mu\text{g mL}^{-1}$ of UR-NP@PEI (with/without DOX) for 2 h and washed with PBS to remove non-internalized nanoparticles. Quantification of doxorubicin in the DOX-Platform was carried out as described for DOX-UR-NPs@PEI, dispersing the DOX-Platform in 95% ethanol under sonication (therefore, releasing the cell content, including the nanoparticles, to the ethanolic solution) and measuring the fluorescence.

Cell viability was evaluated after 1 and 3 days by Alamar Blue assay, following the manufacturer's instructions: 10 % of the reagent was added to the culture medium with the DMSCs and incubated at 37 °C for 1 h. Then, fluorescence at λ_{exc} 560, λ_{em} 590 nm was measured in a spectrofluorimeter plate reader. Cell viability was then analyzed as a percentage of the control wells (DMSCs not exposed to DOX-Nanoparticles).

Migration capacity towards mammary tumor homogenate. Animal Care was carried out in accordance with the Royal Decree 223/1988 (BOE 8, 18) and the Ministerial Order of 13 October 1989 (BOE 8) regarding the protection of experimental animals, as well as with the European Council Directive 86/609/EEC and approved by the Committee of Ethics and Animal Welfare (CEBA) from Hospital Universitario 12 de Octubre. N-nitroso-N-methylurea (NMU) tumors were induced in 45-day-old Sprague-Dawley female rats according to our previously published protocol⁴⁶. The tumors were dissected out from the animals, immediately frozen in liquid nitrogen and subsequently stored at -80 °C until further use. Homogenates from those tumors were performed at 4 °C as we previously described.³⁴ The protein concentration was measured using the Lowry protein assay kit (Biorad, Spain) following the manufacturer's instructions.

The migration capacity of the engineered platform towards tumor homogenate was performed using Millicell culture plate inserts with 8 μm pore polycarbonate membranes (Merk Millipore, Spain) in 24-well plates. 1.5×10^5 DMSCs containing UR-NPs@PEI (with/without DOX) in 300 μL of serum-free DMEM were seeded in the insert. Tumor homogenate (5 mg mL^{-1} of protein concentration) was added in the well below. Migration medium (serum-free DMEM) without tissue was used as a negative control. Migration was assessed at 24 h by the CytoSelect 24-Well Cell Migration Assay (8 μm , Colorimetric, Cell Biolabs, Bionova Científica, S.L., Spain). Non-migratory cells were removed from the top of the membrane and migratory cells on the bottom of the polycarbonate membrane were stained with the Cell Stain Solution and quantified according to manufacturer's instructions. Migratory cells were visualized (three individual fields per insert) using a

light microscope under x40 magnification objective. Color of stained cells was subsequently extracted with the Extraction Solution, and quantified by absorbance at 560 nm using the multimodal plate reader Enspire (Perkin Elmer). All experiments were done as a minimum in triplicate.

In vitro co-culture experiments. DMSCs or the engineered DOX-Platform (UR-NPs@PEI inside DMSCs, with doxorubicin) were co-cultured with NMU rat mammary cancer cells (ATCC, LGC Standards S.L.U., Spain). NMU cells were cultured in 24 well plates at a density of 20,000 cells per well 24 h before the experiment was carried out. DMSCs were incubated with DOX-UR-NPs@PEI as previously described. After washing non internalized nanoparticles, DMSCs (with and without NPs) were trypsinized and ultrasound was applied to some of the DMSCs suspensions (1 MHz, 3 W cm^{-2} , 5 min continuous application). Then, DMSCs with or without DOX-NPs (and with or without US exposure) were seeded in Transwell® culture inserts (0.4 μm pore, polycarbonate membranes, tissue cultured treated, Costar®), in the same plate containing NMU cells, in two different DMSCs:NMU ratios (1:2 and 1:5). After 1 and 2 days, the inserts were removed and NMU cells viability was analyzed by Alamar Blue test, as previously described.

Ultrasonic experiments.

For the *in vial* release experiments, the US experiments were performed in a commercial laboratory ultrasound apparatus (RBI, France), working at 1.3 MHz and 100 W during 10 min, in similar conditions to those described in our previous work.¹⁵

For the *in vivo* and *in vitro* intracellular cargo release experiments, a commercial ultrasound apparatus for application in physical therapy was used (New Pocket Sonovit, New Age Italia Srl, Italy). The parameters selected were: 1 MHz, 3 W cm^{-2} , continuous application, 5-10 min. In the *in vitro* intracellular experiments, ultrasound was applied from the top of a filled culture well through a latex membrane (ultrasound transmission gel was placed between the transducer and the latex membrane).

Acknowledgements

Authors thank the funding from the European Research Council through the Advanced Grant VERDI (ERC-2015 AdG Proposal no. 694160). Financial support from Ministerio de Economía y Competitividad, (MEC), Spain (Project MAT2015-64831-R) is gratefully acknowledged. JL Paris gratefully acknowledges MEC, Spain, for his PhD grant (BES-2013-064182). This work was sponsored by grants PI11/00581; PI13/00045; PI15/01803 (Ministry of Economy, Industry and Competitiveness) and cofunded by the European Regional Development Fund, and approved by the Ethics Committee of our Institution; MULTIMAT-CHALLENGE (S2013/MIT-2862) from Comunidad de Madrid and the Neurosciences and Aging Foundation, the Francisco Soria Melguizo Foundation, Octopharma and Parkinson Madrid (PI2012/0032 and PI2013/0116).

Notes and references

- 1 S. Mura, J. Nicolas and P. Couvreur, *Nat. Mater.*, 2013, **12**, 991–1003.
- 2 A. Baeza, M. Colilla and M. Vallet-Regí, *Expert Opin. Drug Deliv.*, 2015, **12**, 319–337.
- 3 M. Vallet-Regí, A. Rámila, R. P. del Real and J. Pérez-Pariente, *Chem. Mater.*, 2001, **13**, 308–311.
- 4 Z. Li, J. C. Barnes, a Bosoy, J. F. Stoddart and J. I. Zink, *Chem. Soc. Rev.*, 2012, **41**, 2590–2605.
- 5 A. Baeza, M. Manzano, M. Colilla and M. Vallet-Regí, *Biomater. Sci.*, 2016, **4**, 803–813.
- 6 Z. Li, D. L. Clemens, B.-Y. Lee, B. J. Dillon, M. A. Horwitz and J. I. Zink, *ACS Nano*, 2015, **9**, 10778–10789.
- 7 Z. Luo, K. Cai, Y. Hu, L. Zhao, P. Liu, L. Duan and W. Yang, *Angew. Chem. Int. Ed. Engl.*, 2011, **50**, 640–643.
- 8 A. Popat, B. P. Ross, J. Liu, S. Jambhrunkar, F. Kleitz and S. Z. Qiao, *Angew. Chemie Int. Ed.*, 2012, **51**, 12486–12489.
- 9 Y.-Z. You, K. K. Kalebaila and S. L. Brock, *Chem. Mater.*, 2008, **20**, 3354–3359.
- 10 M. Martínez-Carmona, A. Baeza, M. a. Rodríguez-Milla, J. García-Castro and M. Vallet-Regí, *J. Mater. Chem. B*, 2015, **3**, 5746–5752.
- 11 J. Liu, C. Detrembleur, M.-C. De Pauw-Gillet, S. Mornet, C. Jérôme and E. Duguet, *Small*, 2015, **11**, 2323–2332.
- 12 E. Guisasola, A. Baeza, M. Talelli, D. Arcos, M. Moros, J. M. de la Fuente and M. Vallet-Regí, *Langmuir*, 2015, **31**, 12777–12782.
- 13 S. Carregal-Romero, P. Guardia, X. Yu, R. Hartmann, T. Pellegrino and W. J. Parak, *Nanoscale*, 2015, **7**, 570–576.
- 14 S.-F. Lee, X.-M. Zhu, Y.-X. J. Wang, S.-H. Xuan, Q. You, W.-H. Chan, C.-H. Wong, F. Wang, J. C. Yu, C. H. K. Cheng and K. C.-F. Leung, *ACS Appl. Mater. Interfaces*, 2013, **5**, 1566–1574.
- 15 J. L. Paris, M. V. Cabanas, M. Manzano and M. Vallet-Regí, *ACS Nano*, 2015, **9**, 11023–11033.
- 16 D. Roy, J. N. Cambre and B. S. Sumerlin, *Prog. Polym. Sci.*, 2010, **35**, 278–301.
- 17 A. P. Blum, J. K. Kammeyer, A. M. Rush, C. E. Callmann, M. E. Hahn and N. C. Gianneschi, *J. Am. Chem. Soc.*, 2015, **137**, 2140–2154.
- 18 H. Hosoya, A. S. Dobroff, W. H. P. Driessen, V. Cristini, L. M. Brinker, F. I. Staquicini, M. Cardó-Vila, S. D'Angelo, F. Ferrara, B. Proneth, Y.-S. Lin, D. R. Dunphy, P. Dogra, M. P. Melancon, R. J. Stafford, K. Miyazono, J. G. Gelovani, K. Kataoka, C. J. Brinker, R. L. Sidman, W. Arap and R. Pasqualini, *Proc. Natl. Acad. Sci.*, 2016, **113**, 1877–1882.
- 19 N. Bertrand, J. Wu, X. Xu, N. Kamaly and O. C. Farokhzad, *Adv. Drug Deliv. Rev.*, 2014, **66**, 2–25.
- 20 J. Fang, H. Nakamura and H. Maeda, *Adv. Drug Deliv. Rev.*, 2011, **63**, 136–51.
- 21 H. Maeda, H. Nakamura and J. Fang, *Adv. Drug Deliv. Rev.*, 2013, **65**, 71–79.
- 22 J. W. Nichols and Y. H. Bae, *Nano Today*, 2012, **7**, 606–618.
- 23 I. K. Kwon, S. C. Lee, B. Han and K. Park, *J. Control. Release*, 2012, **164**, 108–14.
- 24 S. Wilhelm, A. J. Tavares, Q. Dai, S. Ohta, J. Audet, H. F. Dvorak and W. C. W. Chan, *Nat. Rev. Mater.*, 2016, **1**, 16014.
- 25 F. Ratto, S. Centi, C. Avigo, C. Borri, F. Tatini, L. Cavigli, C. Kusmic, B. Lelli, S. Lai, S. Colagrande, F. Faita, L. Menichetti and R. Pini, *Adv. Funct. Mater.*, 2016, **26**, 7178–7185.
- 26 Z. Gao, L. Zhang, J. Hu and Y. Sun, *Nanomedicine Nanotechnology, Biol. Med.*, 2013, **9**, 174–184.
- 27 J. M. Karp and G. S. Leng Teo, *Cell Stem Cell*, 2009, **4**, 206–16.
- 28 Y.-L. Hu, Y.-H. Fu, Y. Tabata and J.-Q. Gao, *J. Control. Release*, 2010, **147**, 154–62.
- 29 M. Roger, A. Clavreul, M.-C. Venier-Julienne, C. Passirani, L. Sindji, P. Schiller, C. Montero-Menei and P. Menei, *Biomaterials*, 2010, **31**, 8393–401.
- 30 L. Kucerova, V. Altanerova, M. Matuskova, S. Tyciakova and C. Altaner, *Cancer Res.*, 2007, **67**, 6304–6313.
- 31 L. S. Sasportas, R. Kasmieh, H. Wakimoto, S. Hingtgen, J. A. J. M. van de Water, G. Mohapatra, J. L. Figueiredo, R. L. Martuza, R. Weissleder and K. Shah, *Proc. Natl. Acad. Sci.*, 2009, **106**, 4822–4827.
- 32 H. Motani, C. Schichor and T. T. Lah, *Cancer*, 2010, **116**, 2519–2530.
- 33 M. I. Macias, J. Grande, A. Moreno, I. Domínguez, R. Bornstein and A. I. Flores, *Am. J. Obstet. Gynecol.*, 2010, **203**, 495.e9–495.e23.
- 34 I. Vegh, M. Grau, M. Gracia, J. Grande, P. de la Torre and A. I. Flores, *Cancer Gene Ther.*, 2013, **20**, 8–16.
- 35 J. L. Paris, P. D. La Torre, M. Manzano, M. V. Cabañas, A. I. Flores and M. Vallet-Regí, *Acta Biomater.*, 2016, **33**, 275–282.
- 36 J. B. Engel, A. V. Schally, S. Buchholz, S. Seitz, G. Emons and O. Ortman, *Arch. Gynecol. Obstet.*, 2012, **286**, 437–442.
- 37 C. E. Soma, C. Dubernet, G. Barratt, F. Nemati, M. Appel, S. Benita and P. Couvreur, *Pharm. Res.*, 1999, **16**, 1710–1716.
- 38 V. V. Padma, *BioMedicine*, 2015, **5**, 19.
- 39 C. J. Springer and I. Niculescu-Duvaz, *J. Clin. Invest.*, 2000, **105**, 1161–1167.
- 40 C. Peters and S. Brown, *Biosci. Rep.*, 2015, **35**, e00225–e00225.
- 41 H. Meng, M. Xue, T. Xia, Y.-L. Zhao, F. Tamanoi, J. F. Stoddart, J. I. Zink and A. E. Nel, *J. Am. Chem. Soc.*, 2010, **132**, 12690–12697.
- 42 S. Wang, P. Huang and X. Chen, *Adv. Mater.*, 2016, **28**, 7340–7364.
- 43 T. Xia, M. Kovochich, M. Liong, H. Meng, S. Kabehie, S. George, J. I. Zink and A. E. Nel, *ACS Nano*, 2009, **3**, 3273–3286.
- 44 X. Li, Y. Chen, M. Wang, Y. Ma, W. Xia and H. Gu, *Biomaterials*, 2013, **34**, 1391–1401.
- 45 J.-T. Lee, M. C. George, J. S. Moore and P. V Braun, *J. Am. Chem. Soc.*, 2009, **131**, 11294–5.
- 46 I. Vegh and R. E. de Salamanca, *J. Carcinog.*, 2007, **6**, 18.